

Cocaine Blocks Effects of Hunger Hormone, Ghrelin, Via Interaction with Neuronal Sigma-1 Receptors

David Aguinaga, ^{1,2}

Mireia Medrano, ^{1,2}

Arnau Cordoní, ³

Mireia Jiménez-Rosés, ³

Edgar Angelats, ^{1,2}

Mireia Casanovas, ^{1,2}

Ignacio Vega-Quiroga, ⁴

Enric I. Canela, ^{1,2}

Milos Petrovic, ⁵

Katia Gysling, ⁴

Leonardo Pardo, ³

Rafael **AQ1** Franco, ^{1,2,7✉}

Phone +34 934021213

Email rfranco123@gmail.com

Email rfranco@ub.edu

Gemma Navarro, ^{1,6,7✉}

Phone +34 934021213

Email dimartts@hotmail.com

¹ Centro de Investigación en Red, Enfermedades Neurodegenerativas

(CIBERNED), Instituto de Salud Carlos III, Madrid, Spain

² Department of Biochemistry and Molecular Biomedicine, School of Biology, Universitat de Barcelona, Barcelona, Spain

³ Laboratori de Medicina Computacional, Unitat de Bioestadística, Facultat de Medicina, Universitat Autònoma de Barcelona, 08193 Bellaterra, Spain

⁴ Department of Cellular and Molecular Biology, Faculty of Biological Sciences, Pontificia Universidad Católica de Chile, Santiago, Chile

⁵ School of Pharmacy and Biomedical Sciences, University of Central Lancashire, Preston, PR1 2HE UK

⁶ Department of Biochemistry and Physiology, Faculty of Pharmacy, Universitat de Barcelona, Barcelona, Spain

⁷ School of Biology, Universitat de Barcelona, Diagonal 643, 08028 Barcelona, Spain

Received: 1 December 2017 / Accepted: 21 May 2018

Abstract

Despite ancient knowledge on cocaine appetite-suppressant action, the molecular basis of **such fact** ~~hunger-prevention~~ remains unknown. Addiction/eating disorders (e.g., binge eating, anorexia, bulimia) share a central control involving reward circuits. However, we here show that the sigma-1 receptor (σ_1R) mediates cocaine anorectic effects by interacting in neurons with growth/hormone/secretagogue (ghrelin) receptors. Cocaine increases colocalization of σ_1R and GHS-R1a at the cell surface. Moreover, in transfected HEK-293T and neuroblastoma SH-SY5Y cells, and in primary neuronal cultures, pretreatment with cocaine or a σ_1R agonist inhibited ghrelin-mediated signaling, in a similar manner as the GHS-R1a antagonist YIL-781. Results were similar in G protein-dependent (cAMP accumulation and calcium release) and in partly dependent or **partly** independent (ERK1/2 phosphorylation and label-free) assays. **We provide solid evidence for direct**

interaction between receptors and the functional consequences, as well as ~~Apart from solid evidence of direct interaction between receptors and the functional consequences, the paper provides~~ a reliable structural model of the macromolecular σ_1 R-GHS-R1a complex, which arises as a key piece in the puzzle of the events linking cocaine consumption and appetitive/consummatory behaviors.

Keywords

Neuroendocrine
Drug addiction
Receptor heteromer
G protein-coupled heteroreceptor complex
Functional selectivity
Cross-regulation

Rafael Franco and Gemma Navarro contributed equally to this work.

Electronic supplementary material

The online version of this article (<https://doi.org/10.1007/s12035-018-1140-7>) contains supplementary material, which is available to authorized users.

Introduction

Used today as a recreational drug, cocaine was first consumed by humans in the form of ~~Cocaa~~ coca leaves. Indigenous peoples of South America, especially those living at higher altitude, were aware that chewing ~~Cocaa~~ coca leaves ~~was key for keeping~~ helped to keep their life style. For example, ~~Cocaa~~ *Erythroxylum coca* was used to facilitate traversing long distances across the Andes with reduced weight and little food. Despite such ancient knowledge, i.e., the appetite suppressant action of cocaine, the molecular basis of hunger prevention remains unknown. This report was undertaken to test the hypothesis of whether the well-known anorexigenic effect of cocaine is mediated by growth hormone secretagogue (GHS) receptors, also known as ghrelin receptors, which are ~~keys~~ **players** in the central control of food/energy intake [1].

Ghrelin, the “hunger” endocrine hormone, is involved in the control of food intake and energy homeostasis [2]. Its action is mediated by, up-to-date, only one specific ghrelin receptor that belongs to the superfamily of G protein-coupled receptors (GPCRs). In humans, ~~this receptor has two isoforms produced by~~ alternative splicing ~~leads to~~: isoform 1a that contains seven transmembrane (TM) ~~domains helices~~ (GHS-R1a, 366 amino acids) and isoform 1b that lacks ~~6 and 7 TM domains-6-and-7 helices~~ (GHS-R1b, 289 amino acids) [3, 4, 5]. These TM domains are required for ligand binding and coupling to heterotrimeric G proteins and, therefore, ghrelin cannot signal via ~~the~~ GHS-R1b ~~receptors isoform~~ [6]. GHS-R1b seems to serve as a modulator of GHS-R1a surface expression and signaling [7]. In fact, GHS-R1b is expressed in the same cells as GHS-R1a, and both isoforms interact to form heteromer receptor signaling units [6]. We have previously shown that GHS-R1b guides surface expression of functional GHS-R1a, acting as a dual modulator: low relative GHS-R1b expression potentiates GHS-R1a function, while high relative GHS-R1b expression inhibits GHS-R1a function [7]. GHS-R1b negatively influences ghrelin action by allosteric interactions ~~within~~ the GHS-R1a-GHS-R1b heteromer that reduce the efficacy of the hormone [6, 8]. Although the purified GHS-R1a, assembled into lipid discs ~~and-it~~ is reportedly coupled to $G_{q/11}$ [9], the receptor may also couple to non- $G_{q/11}$ heterotrimeric G proteins (www.guidetopharmacology.org). Indeed, we previously found preferential $G_{i/o}$ coupling of the GHS-R1a-GHS-R1b complex in HEK-293T cells and preferential $G_{s/olf}$ coupling in both striatal and hippocampal neurons in culture [7]. Heteromerization of GHS-R1a and GHS-R1b in heterologous expression systems is often needed for proper ghrelin-induced signaling. It should be noted that ghrelin receptors may form direct protein-protein interactions with a variety of GPCRs, inter alia with dopamine, melanocortin, prostanoid, serotonin, somatostatin, neurotensin, and GPR83 receptors [10]; see www.gpcr-hetnet.com and references therein.

The sigma-1 receptor (σ_1R) is an atypical membrane protein, whose exact function remains unknown. It has been proposed that it functions as a pluripotent cell function modulator in living cells [11] ~~that~~ ~~and~~ is attracting a lot of interest due to its potential as a target against neuropathic pain [12, 13, 14]. While its physiological function remains elusive and the endogenous ligand is yet to be discovered, σ_1R is a protein target for cocaine [15, 16, 17]. Drugs

blocking the interaction of cocaine with σ_1 R have been proposed to reduce drug-seeking behavior [18]. σ_1 R-mediated cocaine actions in the central nervous system are dependent on its interactions with GPCRs. For instance, we have identified that cocaine binding to σ_1 R potentiates dopamine D_1 R-mediated adenylate cyclase signaling [19, 20] and inhibits D_2 R-mediated signaling in striatal neurons [20]. ~~This~~ **These actions** disrupts the delicate balance between inputs of reward seeking controlled by D_1 R-containing neurons and inputs of aversion coming from D_2 R-containing neurons. In addition, cocaine binding to σ_1 R also induces disruption of the orexin and corticotropin-releasing factor receptor negative cross-talk, playing an important role in the stress-induced cocaine-seeking behavior [21].

We show in this manuscript that σ_1 R interacts with and modulates the activity of GHS-R1a, indicating a ~~a receptor interplay not non-~~previously suspected **receptor interplay**. Moreover, because structural information on GPCR ~~macromolecular~~ **homomeric** complexes already exist [22] and the crystal structure of σ_1 R has been recently elucidated [23], we have devised ~~the~~ **a molecular architecture arrangement consisting** of the GHS-R1a-GHS-R1b heteromer in complex with σ_1 R. We have taken advantage of the recent knowledge showing that σ_1 R arranges as a homotrimer (each protomer with a single TM). We used synthetic peptides with the amino acid sequences from the TM helices of GHS-R1a, together with bimolecular fluorescence complementation assays and computer modeling, to find the oligomerization interfaces between GHS-R1a, GHS-R1b, and σ_1 R, and to propose a structural model of the macromolecular complex.

Materials and Methods

Reagents

Cocaine-chlorhydrate was provided by the Spanish *Agencia del Medicamento* (ref no.: 2003C00220). σ_1 R (PRE-084), GHS-R1a (ghrelin and YIL-781), and A_1 adenosine receptor (L-phenylisopropyl adenosine, R-PIA, and 1,3-dipropyl-8-cyclopentylxanthine, DPCPX) ligands were purchased from Tocris, Bristol, UK. Cocaine-chlorhydrate used for the acute and chronic administration was donated by the National Institute of Drug Abuse, USA, to K. Gysling, Chile.

Fusion Proteins and Expression Vectors

Sequences encoding amino acid residues 1–155 and 155–238 of the Venus variant of yellow fluorescence protein (Venus) were subcloned in the pcDNA3.1 vector to obtain complementary Venus N- and C-hemiproteins. Human cDNAs for GHS-R1a, GHS-R1b, or σ_1 R were amplified without their stop codons using sense and antisense primers harboring: EcoRI and KpnI sites to be subcloned in pcDNA3.1RLuc vector (pRLuc-N1 PerkinElmer, Wellesley, MA) or in a GFP²-containing vector (p-GFP², Packard BioScience, Meriden, CT) to provide σ_1 R-Rluc, GHS-R1a-Rluc, GHS-R1a-YFP, σ_1 R-YFP, or GHS-R1a-GFP² plasmids. Human cDNA for A_{2A}R was subcloned into p-GFP² vector harboring HindIII and BamHI sites to provide the encoding A_{2A}-GFP² plasmid. For bimolecular fluorescence complementation (BiFC) experiments, cDNA for GHS-R1b, GHS-R1a, and σ_1 R were subcloned into pcDNA3.1-nVenus and pcDNA3.1-cVenus harboring EcoRI and KpnI sites to provide plasmids encoding GHS-R1b-nYFP, GHS-R1b-cYFP, GHS-R1a-nYFP, and σ_1 R-cYFP.

Cell Lines, Neuronal Primary Cultures, and Transient Transfection

HEK-293T human embryonic kidney cells were grown in Dulbecco's modified Eagle's medium (DMEM) (Gibco) supplemented with 2 mM L-glutamine, 100 µg/ml sodium pyruvate, 100 U/ml penicillin/streptomycin, MEM Non-Essential Amino Acid Solution (1/100) and 5% (v/v) heat-inactivated fetal bovine serum (FBS) (all supplements were from Invitrogen, Paisley, Scotland, UK). Primary cultures of striatal neurons were obtained from fetal Sprague Dawley rats of 19 days. Cells were isolated as described in Hradsky et al. (2013) and plated at a confluence of 40,000 cells/0.32 cm². Cells were maintained for 12 days in Neurobasal medium supplemented with 2 mM L-glutamine, 100 U/ml penicillin/streptomycin, and 2% (v/v) B27 supplement (GIBCO) in 6-well microplates. Cells were transiently transfected with the corresponding cDNAs using the PEI (PolyEthylenImine, Sigma-Aldrich, St. Louis, MO, USA) method or, in the case of the anti- σ_1 R siRNA, with Lipofectamine 2000 (Thermo Fisher Scientific). After transfection, cells were incubated in serum-free medium which was replaced by complete medium after 4 h. Experiments were carried out 48 h later (unless otherwise indicated).

AQ2

Immunocytochemistry

HEK-293T cells were fixed in 4% paraformaldehyde for 15 min and washed with PBS containing 20 mM glycine to quench free aldehyde groups. After permeabilization with PBS-glycine buffer containing 0.2% Triton X-100 for 5 min, cells were blocked with PBS containing 1% bovine serum albumin (1 h at room temperature). σ_1 R-YFP was detected by its own fluorescence (wavelength 530 nm), and Rluc-containing proteins were stained using a mouse monoclonal anti-Rluc antibody (1/200, 1 h, room temperature, Millipore, CA, USA) and a Cyn3-conjugated donkey anti-mouse antibody (1/200, Jackson ImmunoResearch Laboratories, West Grove, PA, USA). Nuclei were stained with Hoechst (1/100, Sigma-Aldrich, St. Louis, USA) and samples were mounted with Mowiol 30% (Calbiochem) and observed in a Leica SP2 confocal microscope (Leica Microsystems, Mannheim, Germany).

Resonance Energy Transfer

For bioluminescence energy transfer (BRET) assays, HEK-293T cells were transiently transfected with a constant amount of cDNA for σ_1 R-Rluc and increasing amounts of cDNAs for GHS-R1a-GFP² or A_{2A}-GFP². To normalize the number of cells, protein concentration was determined using a Bradford assay kit (Bio-Rad, Munich, Germany) using bovine serum albumin dilutions as standards. To quantify fluorescence, cell suspensions were distributed in 96-well microplates (black with transparent bottom), and fluorescence was read in a Fluostar Optima Fluorimeter (BMG Labtech, Offenburg, Germany) equipped with a high-energy xenon flash lamp, using a 10 nm bandwidth excitation filter (400 nm). For BRET measurements, cell suspensions (20 μ g protein) were distributed in 96-well white microplates (Corning 3600, Corning, NY), and 5 μ M DeepBlueC (Molecular Probes, Eugene, OR) was added right before BRET signal acquisition using a Mithras LB 940 reader (Berthold Technologies, DLReady, Germany). To quantify receptor-Rluc expression, luminescence readings were performed after 10 min of adding 5 μ M coelenterazine H. Net BRET is defined as [(long-wavelength emission)/(short-wavelength emission)] – C_f , where C_f corresponds to [(long-wavelength emission)/(short-wavelength emission)] for the Rluc protein when expressed individually. For bimolecular complementation (BiFC) assays, HEK-293T cells were transiently transfected

with a constant amount of cDNA encoding for proteins fused to nVenus or cVenus and incubated for 4 h in complete DMEM containing the interfering TAT peptides (with similar sequences to those in TM1 to TM7 of GHS-R1a; see supplementary Table 1 for sequences). YFP resulting from complementation was detected by placing cells (20 μ g protein) in 96-well microplates (black plates with a transparent bottom) and reading the fluorescence in a Fluostar Optima Fluorimeter (BMG Labtech, Offenburg, Germany) using a 30-nm bandwidth excitation filter (485 nm).

AQ3

Cytosolic cAMP Determination

Forskolin dose-response curves in different density of cells were performed to select the most appropriate conditions of the assay, which resulted in 5000 HEK-293T cells, 7500 neurons, and 0.5 μ M forskolin. Subsequently, assays were performed in medium containing 50 μ M zardaverine, placing cells in 384-well microplates. This was done by the preincubation with reagents (the σ_1 R agonist, PRE-084, the GHS-R1a antagonist, YIL-781, or cocaine) for 15 min, followed by ghrelin addition (100-nM final concentration), and after 15 min incubation period, 50 μ M forskolin was added. Readings were performed 15 min later using a homogeneous time-resolved fluorescence energy transfer (HTRF) method requiring the Lance Ultra cAMP kit (PerkinElmer) and fluorescence readings (at 665 nm) in a PHERAstar Flagship microplate reader equipped with an HTRF optical module (BMG Labtech).

MAPK Activation

To determine ERK1/2 phosphorylation, 40,000 HEK-293 cells/well or 50,000 neurons/well were plated in transparent Deltalab 96-well microplates and kept in the incubator for 48 h. The medium was substituted by serum-free DMEM medium 2 to 4 h before starting the experiment. Before the addition of 100 nM, ghrelin cells were pretreated (10 min at 25 °C) in serum-free medium with different reagents (the σ_1 R agonist, PRE-084, the GHS-R1a antagonist, YIL-781, or cocaine). After 7 min of ghrelin-induced activation, cells were washed twice with cold PBS before the addition of 30 μ L of lysis buffer (20 min). Supernatants (10 μ L) were placed in white ProxiPlate 384-well microplates, and ERK1/2 phosphorylation was determined using the AlphaScreen®SureFire® kit

(Perkin Elmer) and the EnSpire® Multimode Plate Reader (PerkinElmer, Waltham, MA, USA).

Intracellular Calcium Mobilization

HEK-293T cells were co-transfected with cDNA(s) for receptor(s) and 1 μg cDNA for the calmodulin-based calcium sensor, GCaMP6 (Chen et al. 2013). Forty-eight hours after transfection, cells were detached using Mg^{2+} -free Locke's buffer pH 7.4 (154 mM NaCl, 5.6 mM KCl, 3.6 mM NaHCO_3 , 2.3 mM CaCl_2 , 5.6 mM glucose, and 5 mM HEPES) supplemented with 10 μM glycine. One hundred fifty thousand cells per well were plated in 96-well black, clear bottom, microtiter plates. Then, cells were incubated with the $\sigma_1\text{R}$ agonist, PRE-084, the GHS-R1a antagonist, YIL-781, or cocaine for 10 min before ghrelin 100-nM addition. Upon excitation at 488 nm, real-time 515-nm fluorescence emission due to calcium-ion-complexed GCaMP6 was recorded on the EnSpire® Multimode Plate Reader (every 5 s, 100 flashes per well).

Label-Free Dynamic Mass Redistribution Assays

HEK-293T cells and neuronal primary cultures were seeded in 384-well sensor microplates to obtain 70–80% confluent monolayers constituted by 10,000 HEK-293T cells or 14,000 neurons per well. Before the assay, cells were washed twice with assay buffer (HBSS with 20 mM HEPES and 0.1% DMSO, pH 7.15) and incubated for 2 h in 40 μL /well of assay-buffer in the reader at 24 °C. Hereafter, the sensor plate was scanned, and a baseline optical signature was recorded before adding 10 μL of cocaine (30 μM), PRE-084 (100 nM), or YIL-781 (2 μM) for 30 min followed by ghrelin addition. All compounds were dissolved in assay buffer. Then, dynamic mass redistribution (DMR) responses were monitored for at least 3600 s using an EnSpire® Multimode Plate Reader (PerkinElmer, Waltham, MA, USA). Sensitive measurements of changes in local optical density mimicking cellular mass movements induced upon receptor activation were detected using EnSpire Workstation Software v 4.10.

Proximity Ligation Assay

For proximity ligation assays (PLAs), primary cultures of striatal neurons were fixed in 4% paraformaldehyde for 30 min and permeabilized in PBS containing 0.05% Triton X-100 (15 min). After 1 h incubation at 37 °C with the blocking

solution, primary cultures were incubated overnight with anti- σ_1 R (1/100, Santa Cruz Biotechnology, Dallas, USA), and anti-GHS-R1a antibody (1/100, AbCam, Cambridge, UK) in the presence of Hoechst (1/100, Sigma-Aldrich, St. Louis, USA) to stain nuclei. Cells were processed using the PLA probes that bind to the primary antibodies (Duolink II PLA probe anti-Mouse plus and Duolink II PLA probe anti-Goat minus) and heteroreceptor complex formation was detected using the Duolink II in situ PLA detection Kit (OLink; Bioscience, Uppsala, Sweden). Images were taken in a Leica SP2 confocal microscope (Leica Microsystems, Mannheim, Germany). For each field of view, a stack of two channels (one per staining), and four to six Z stacks with a step size of 1 μ m were acquired. Quantification of the number of cells containing one or more red dots versus total cells (blue nuclei) and of the number of red dots/cell-containing dots:r ratio was conducted using a dedicated software known as Duolink ImageTool (ref: DUO90806, Sigma-Olink). This software has been developed for PLA signals and cell nuclei quantification in images generated from fluorescence microscopy.

Cocaine Treatment and Fixation Procedure

Male Sprague-Dawley rats weighing 200–220 g were selected for the experiments. Rats were kept in controlled environment with 12-h light-dark cycle at 21 °C room temperature. Food and water were provided ad libitum. All experimental procedures were approved by the Ethics Committee of the Faculty of Biological Sciences of “Pontificia Universidad Católica de Chile” and followed the international guidelines (NIH Guide for the Care and Use of Laboratory Animals). Rats were divided in two groups of experimental series, chronic cocaine-treated rats with respective control (saline) and acute cocaine rats. The chronic cocaine-administration protocol consisted of 15 mg/Kg, i.p. cocaine injections twice per day for 14 days as described by [24], whereas the acute cocaine treatment protocol consisted of two injections of 15 mg/kg, i.p. cocaine, one in the morning and one in the afternoon. Daily administration of cocaine and saline solution was performed in both experimental series at the same time in the morning and afternoon (beginning at 11:00 A.M. and 5:00 P.M.). The day after last cocaine injection, rats were deeply anesthetized with ketamine-xylazine (50–5 mg/kg, respectively) and intracardially perfused with 50 ml of saline, followed by 500 ml of 4% paraformaldehyde (PFA) in phosphate buffer. Then, the animals were guillotined, and the brain was post-

fixed with 4% PFA for 2 h and left in 20% sucrose during 2 days.

Computational Model of the GHS-R1a- σ_1 R Heteromer

The structure of σ_1 R was modeled based on the recently released crystal structure (PDB id 5HK1) [25]. The inactive conformation of human GHS-R1a (UniProt: Q92847) was built using crystal structures of the neurotensin 1 receptor (PDB id 4XES for all parts of the receptor, and PDB id 3ZEV for the C-terminal part of TM7 and helix 8) [26, 27]. The human neurotensin 1 receptor and GHS-R1a share 33% of sequence identity and 51% of sequence similarity. The “active-like” form of GHS-R1a was modeled by incorporating the active features present in the crystal structure of the β_2 -adrenergic receptor in complex with G_s (PDB id 3SN6), **namely the internal halves of TMs 5 and 6** [28]. The “active-like” model of GHS-R1a contains G_i (PDB id 1AGR) [29]. The GHS-R1a homodimer was constructed based on the symmetric TM5/6 protein-protein interface observed in the crystal structure of the μ OR (PDB id 4DKL) [30]. The GHS-R1a- σ_1 R complex was constructed using protein-protein docking with HADDOCK [31], under the imposed experimental restrains that TMs 1 and 2 of GHS-R1a contact the single TM of σ_1 R.

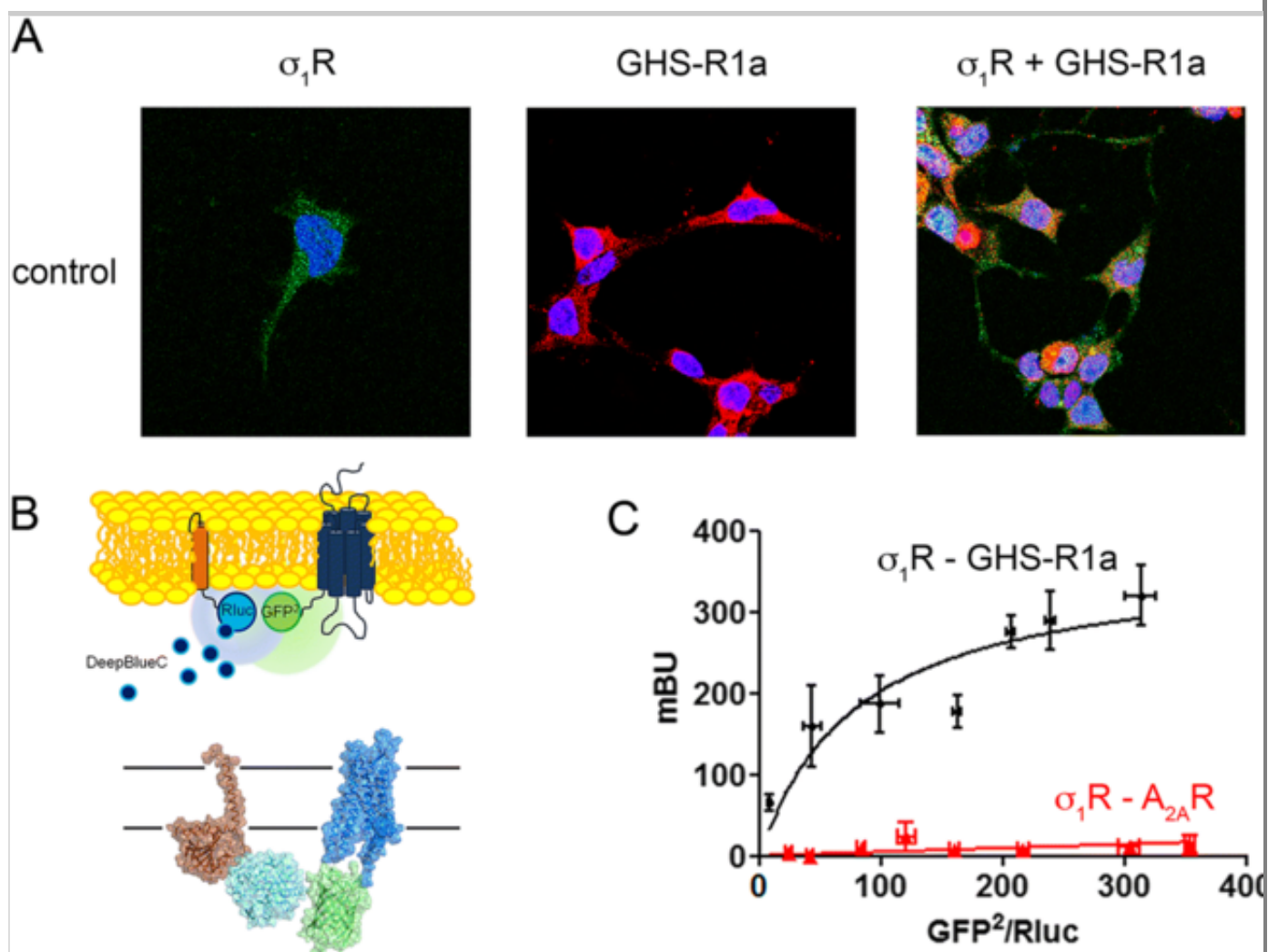
Results

GHS-R1a Forms Heteromeric Complexes with σ_1 R

Immunocytochemical assays were performed to detect whether colocalization between GHS-R1a and σ_1 R occurred in transfected HEK-293T cells. Cells were transfected with cDNAs for σ_1 R fused to YFP (0.75 μ g cDNA) and for GHS-R1a fused to Renilla luciferase (Rluc) (1.66 μ g cDNA). In cells expressing only σ_1 R-YFP, the receptor was detected by YFP fluorescence, identifying σ_1 R-YFP mainly in intracellular structures. In HEK-293T cells expressing GHS-R1a-Rluc, the GHS-R1a was detected by a specific primary anti-Rluc and secondary Cy3 antibodies, **being the receptor was** detected in intracellular structures and at the plasma membrane level. Interestingly, in HEK-293T cells co-expressing σ_1 R-YFP (0.75 μ g cDNA) and GHS-R1a-Rluc (1.66 μ g cDNA), colocalization of both receptors was observed (Fig. 1a).

Fig. 1

GHS-R1a interacts with σ_1 R to form σ_1 R-GHS-R1a heteroreceptor complexes. **a** HEK-293T cells expressing σ_1 R-YFP, GHS-R1a-Rluc, or both were monitored by the YFP fluorescence (green) or using a monoclonal anti-Rluc primary antibody and a cyanine-3-conjugated secondary antibody (red). Colocalization is shown in yellow. Nuclei were stained in blue with Hoechst (1/100). Scale bar 10 μ m. **b** Scheme of the BRET² assay using σ_1 Rluc and GHS-R1a-GFP². **c** BRET occurs in HEK-293T cells transfected with a constant amount of cDNA (0.075 μ g) for σ_1 Rluc and increasing amounts of GHS-R1a-GFP² (from 0.5 to 3 μ g cDNA) or A_{2A} R-GFP² (from 0.5 to 2.5 μ g cDNA) as negative control. Values are the mean (in milliBRET units: mBU) \pm S.E.M. from six to eight different experiments



To identify a potential direct interaction between σ_1 R and GHS-R1a, we developed BRET experiments, transfecting a constant amount of cDNA for σ_1 R-Rluc (0.075 μ g cDNA) and increasing amounts of cDNA for GHS-R1a-GFP²

(0.5 to 3 μg cDNA). A saturation BRET curve was obtained, thus indicating a specific interaction between $\sigma_1\text{R}$ and GHS-1a (BRET_{max} 371 ± 38 mBU, BRET_{50} 68 ± 23) (Fig. 1b, c). In contrast, when adenosine $\text{A}_{2\text{A}}\text{R-GFP}^2$ (0.5 to 2.5 μg cDNA) was used as negative control instead of GHS-R1a receptor, a linear plot with low BRET values was obtained.

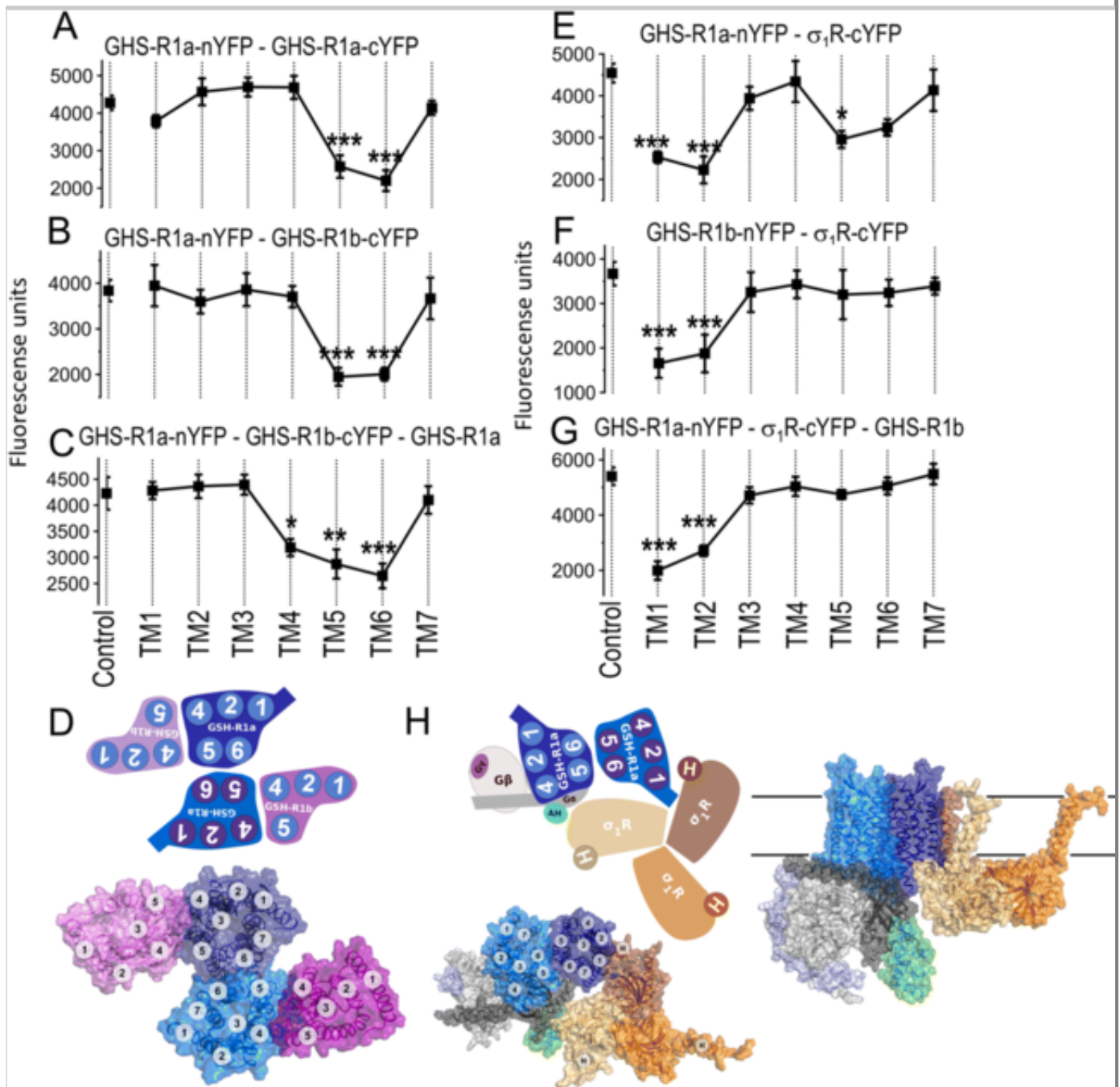
Quaternary Structure of the Heteromeric Complex Between $\sigma_1\text{R}$ and GHS-R1a

We next addressed the quaternary structure of $\sigma_1\text{R}$ -GHS-R1a complexes taking advantage of the recent publication of the crystal structure of $\sigma_1\text{R}$ in a trimeric ~~receptor~~ arrangement. The macromolecular complex cannot be understood without taking into account that the GHS-R1a receptor can form homomeric interactions with GHS-R1a and/or heteromeric interactions with GHS-R1b [6, 7, 8]. Thus, to identify the TM interfaces involved in GHS-R1a-GHS-R1a homodimerization, GHS-R1a-GHS-R1b heterodimerization and their TM-interacting interfaces with $\sigma_1\text{R}$, we used synthetic peptides with the amino acid sequence of individual 1-7 TM ~~domains 1–7~~ helices of GHS-R1a fused to the transactivator of transcription (TAT) peptide (exact sequences are provided in supplementary Table 1). These cell-penetrating peptides interact with the TM domain of membrane proteins and can selectively disrupt interactions between proteins, i.e., GPCR protomers [32, 33]. These peptides were first tested in HEK-293T cells expressing GHS-R1a-nYFP (0.75 μg cDNA) and GHS-R1a-cYFP (0.5 μg cDNA) to explore whether bimolecular fluorescence complementation (BiFC) occurs (approximately ~~4000~~ 4,000 units of fluorescence indicative of the formation of GHS-R1a-homodimer complexes). Notably, in the presence of interference peptides, we observed that the fluorescence decreased by twofold only with TM5 and TM6 peptides (Fig. 2a). These results pointed to the TM 5/6 interface for GHS-R1a-GHS-R1a homodimerization. Similar results were obtained for GHS-R1a-GHS-R1b heterodimerization (TM 5/6 interface, Fig. 2b), despite the fact that GHS-R1b isoform lacks TMs 6 and 7 ~~relative to GHS-R1a~~. Interestingly, when cells were transfected with cDNAs for GHS-R1a-nYFP, GHS-R1b-cYFP, and non-fused GHS-R1a, fluorescence was reduced in the presence of TM4, TM5, and TM6 peptides (Fig. 2c). These results suggest an arrangement of protomers in which homodimerization of GHS-R1a occurs via the TM 5/6 interface, whereas heterodimerization of GHS-R1a and GHS-R1b occurs via the TM 4/5 interface

(Fig. 2d). The fluorescence decrease induced by the TM6 peptide of GHS-R1a (in addition to TM4 and TM5, Fig. 2c) could indicate that this peptide also restricts the interactions with [the](#) TM 4 of GHS-R1b (Fig. 2d).

Fig. 2

Effect of interfering peptides on the σ_1 R-GHS-R1a interaction. **a–c, e–g** BiFC complementation experiments were performed in HEK-293T cells transfected with 0.75 μ g cDNA for GHS-R1a-nYFP and 0.75 μ g cDNA for GHS-R1a-cYFP (**a**), with 0.75 μ g cDNA for GHS-R1a-nYFP and 0.75 μ g cDNA for GHS-R1b-cYFP (**b**), with 0.75 μ g cDNA for GHS-R1a-nYFP and 0.75 μ g cDNA for GHS-R1b-cYFP in the presence of 1.5 μ g cDNA for GHS-R1a-nYFP (**c**), with 0.75 μ g cDNA for GHS-R1a-nYFP and 0.75 μ g cDNA for σ_1 R-cYFP (**e**), with 0.5 μ g cDNA for GHS-R1b-nYFP and 0.5 μ g cDNA for σ_1 R-cYFP (**f**), or with 0.75 μ g cDNA for GHS-R1a-nYFP and 0.75 μ g cDNA for GHS-R1b-cYFP (**g**) in the presence of 1.5 μ g cDNA of GHS-R1a not fused. Prior to fluorescence determination, cells were treated with each of the interfering peptides (TM1 to TM7, 4 μ M) during 4 h. Values are the mean \pm S.E.M. from eight to 10 different experiments. One-way ANOVA followed by Dunnett's *post hoc* test showed a significant effect of treatments versus control conditions. * $p < 0.05$, ** $p < 0.01$, and *** $p < 0.001$. **d** Structural model for the GHS-R1a-GHS-R1b heterotetramer (GHS-R1a protomers: blue, GHS-R1b protomers: purple) viewed from the extracellular side (scheme of the arrangement—top—and three-dimensional model (—bottom—)). **h** (left) Structural model consisting of a GHS-R1a homodimer (GHS-R1a G_α -bound: light blue, GHS-R1a G_α -unbound: dark blue) in complex with a σ_1 R homotrimer (in red, orange, and yellow) coupled to G_i (G_α Ras-like domain: light gray, G_α alpha helical domain: green, G_β : dark gray, and G_γ : purple) viewed from the extracellular side. **h** (right) Same model as in panel **h** (left) but viewed across the plane of the membrane. Proteins are displayed with a transparent surface and a cartoon. TM helices are indicated by circles (1–7 in GHS-R1a, 1–5 in GHSR1b and H in σ_1 R)



Next, we investigated the GHS-R1a TM domains involved in the interaction with σ_1 R. Remarkably, in HEK-293T cells co-expressing GHS-R1a-nYFP (0.75 μ g cDNA) and σ_1 R-cYFP (0.5 μ g cDNA), fluorescence complementation (~~4000~~ 4,000 units, which confirms the formation of GHS-R1a- σ_1 R complexes as shown in confocal images (Supplementary Fig. 1A)) was significantly reduced in the presence of TM1, TM2, or TM5 peptides; a marked tendency without statistical significance in the case of TM6 peptide was also found (Fig. 2e). This clearly indicates the existence of two different interacting interfaces between GHS-R1a and σ_1 R, involving either TM 1/2 or TM 5/6 interfaces of GHS-R1a

and the single TM helix of σ_1 R. When similar experiments were performed with σ_1 R-cYFP (0.5 μ g cDNA) and GHS-R1b-nYFP (0.5 μ g cDNA), the fluorescent signal (~~3500~~ 3,500 units) decreased in the presence of TM1 and TM2 but not TM5 or TM6 peptides (Fig. 2f); ~~it should be noted again that because~~ GHS-R1b lacks TMs 6 and 7 ~~relative to GHS-R1a~~. All members of the GPCR family retain analogous tertiary structures at the seven-helical-bundle domain; thus, we hypothesized that TM 1/2 or TM 5/6 interfaces could be involved in the interaction between the GPCRs and σ_1 R. In addition, GPCR homo/heteromerization must be taken into account to accommodate the σ_1 receptor in the trimeric structure elucidated from structural studies. ~~To obtain data in a more physiological set-up~~ ~~In order to achieve useful data in more physiological conditions~~, HEK-293T cells were transfected with cDNAs for GHS-R1a-nYFP and σ_1 R-cYFP in the presence of non-fused GHS-R1b. As fluorescence complementation (~~5000~~ 5,000 fluorescence units) was reduced only by TM1 and TM2 (Fig. 2g); our ~~conclusion~~ interpretation was that the formation of the GHS-R1a-GHS-R1b heterotetramer via TM 4/5 and TM 5/6 interfaces (Fig. 2d) only permits σ_1 R to interact with GHS-R1a via the free TM 1/2 interface. Proper interference action of TM-TAT peptides was tested by PLA (Supplementary Fig. 1B). In fact, TM1 and TM2 TAT peptides blocked the expression of GHS-R1a- σ_1 R heteromers while ~~the constituted by~~ treatment with the TM7 TAT did not affect the PLA signal.

Using structural details on TM interfaces of GPCR oligomers [22] and the crystal structure of human σ_1 R [23], together with the results from BiFC experiments performed in the absence and presence of disrupting TM peptides, we constructed a computational molecular model (see “Methods”) of the GHS-R1a homodimer in complex with G_i and σ_1 R (Fig. 2h). The model of the GHS-R1a homodimer contains two free TM 4/5 interfaces that would allow binding of two GHS-R1b protomers (Fig. 2d). ~~The crystal structure of σ_1 R, in which the protein arranges as a homotrimer, suggests that the homotrimer may represent the functional unit~~ ~~However, the structural model for σ_1 R favors a homotrimer~~ [23]. Accordingly, we constructed a computational model consisting of the GHS-R1 dimer, a σ_1 R trimer, and a G protein that fits with the requirements of the biochemical data and takes into account all available structural constraints (Fig. 2g; see “Methods”). According to the experiments with GHS-R1a-derived peptides (~~see above~~) ~~above~~, σ_1 R can bind GHS-R1b through the TM1/2 interface

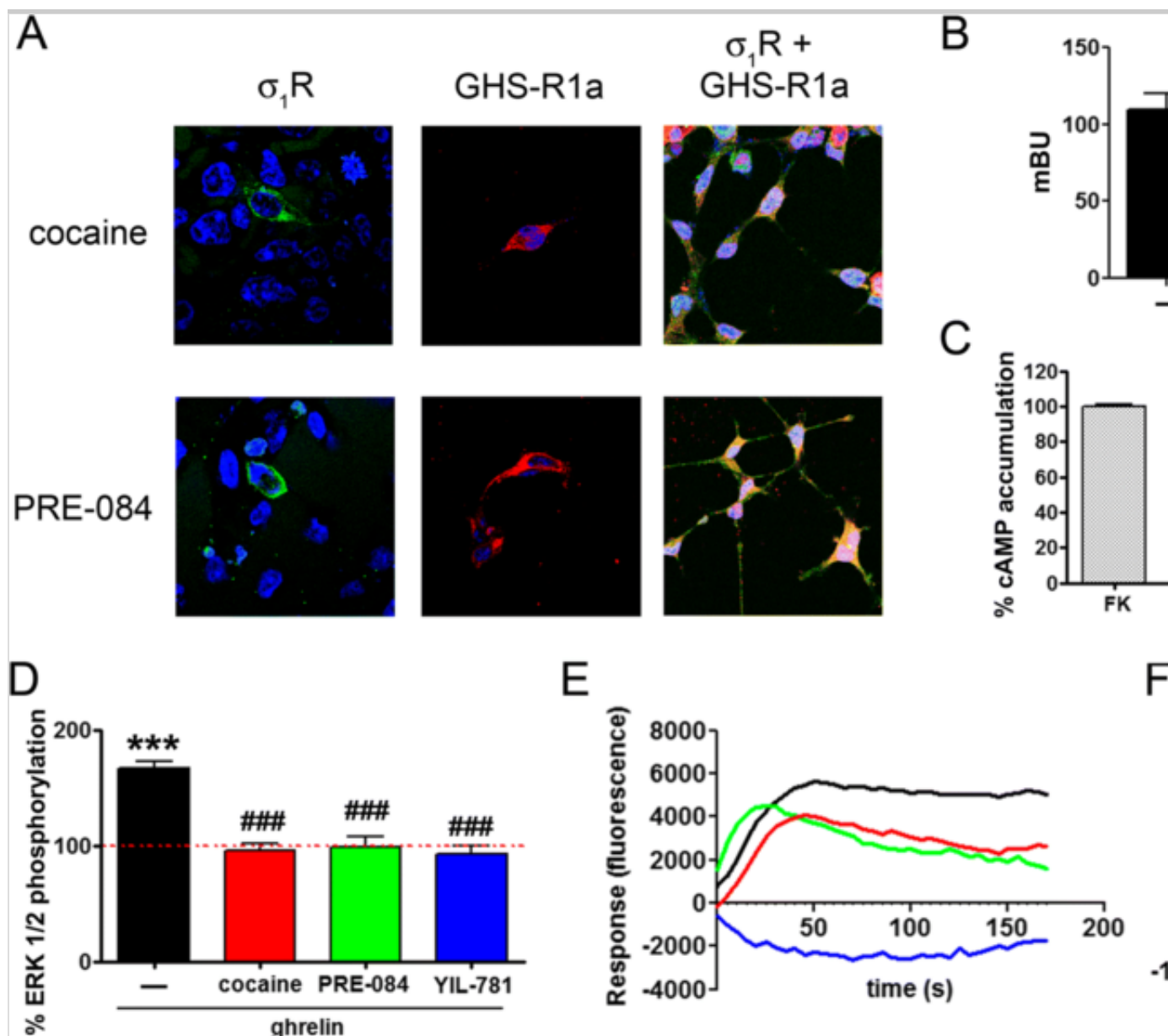
and GHS-R1a through either the TM1/2 or the TM5/6 interfaces. Because GHS-R1a and GHS-R1b also employ the TM5/6 interface for homo-/heterodimerization, we assumed that at normal expression levels, TM1/2 is the **only possible most likely** interface for the GHS-R1- σ_1 R complex, as TM5/6 is occupied by the GHS-R1 homodimer/heterodimer. This model indicates that a single GPCR protomer of GHS-R1a cannot simultaneously bind σ_1 R via the TM 1/2 interface and a G protein due to a steric clash between the $\beta\gamma$ subunits of G_i and the intracellular voluminous C-terminal **domain tail** of σ_1 R, containing a rigid cupin-like β -barrel fold that forms the buried ligand-binding site and the $\beta\gamma$ subunits of G_i (Supplementary Fig. S1). Thus, the minimal functional unit requires a GHS-R1a homodimer in which one protomer binds the G protein, and the second protomer is responsible for the binding of the σ_1 R TM helix (Fig. 2h). Interestingly, this model predicts that the cytoplasmic domain of one protomer of the σ_1 R trimeric structure interacts with the α -subunit of G_i .

Cocaine Increases Colocalization of σ_1 R and GHS-R1a at the Cell Surface

As cocaine binds σ_1 R [34], which establishes direct interactions with ghrelin receptors as shown above, we hypothesized that cocaine affects ghrelin-mediated signals. First, we investigated the effect of cocaine in GHS-R1a expression. Immunocytochemical assays were performed in cells expressing σ_1 R and GHS-R1a after addition of cocaine (30 μ M, 30 min). Figure 3a shows that plasma membrane expression of σ_1 R increased when these cells were treated with a physiologically relevant dose of cocaine [35]. A similar increase was observed when cells were incubated with the σ_1 R agonist PRE-084 (100 nM, 30 min). The expression of GHS-R1a was not modified upon treatment with cocaine or PRE-084 but, interestingly, colocalization of σ_1 R and GHS-R1a at the cell surface increased. Thus, cocaine and the σ_1 R-specific ligand PRE-084 are able to concomitantly affect co-expression of both receptors at the cell surface. Second, we evaluated the effect of cocaine and PRE-084 on the heteromerization of σ_1 R and GHS-R1a. A tendency to increased energy transfer (without reaching statistical significance) was observed in the presence of cocaine (30 μ M) or PRE-084 (100 nM) in HEK-293T cells transfected with 0.075 μ g cDNA for σ_1 R-Rluc and 1.5 μ g cDNA for GHS-R1a-GFP² (Fig. 3b).

Fig. 3

Effects of cocaine on ghrelin-mediated signaling. **a** HEK-293T cells transfected with 0.75 μg cDNA for $\sigma_1\text{R}$ -YFP, 1.66 μg cDNA for GHS-R1a-Rluc, or both were treated with 30 μM cocaine or 100 nM PRE-084, then were monitored by the YFP fluorescence (green) or using a monoclonal anti-Rluc primary antibody and a cyanine-3-conjugated secondary antibody (red). Colocalization is shown in yellow. Nuclei were stained with Hoechst (blue). Scale bar 10 μm . **b** BRET in HEK-293T cells transfected with 0.075 μg cDNA for $\sigma_1\text{R}$ -Rluc and 1.5 μg cDNA for GHS-R1a-GFP² and treated with 30 μM cocaine, 100 nM PRE-084, or vehicle for 30 min. Afterwards, the energy transfer signal was measured. Values are the mean \pm S.E.M. of seven different experiments. One-way ANOVA followed by Dunnett's *post hoc* test did not show any significant effect of treatments versus control. **c–f** HEK-293T cells were transfected with 1.66 μg GHS-R1a cDNA and 0.25 μg GHS-R1b cDNA and treated with 30 μM of cocaine (red), 100 nM of the $\sigma_1\text{R}$ agonist, PRE-084 (green), 2 μM of the GHS-R1a antagonist, YIL-781 (blue), or vehicle (black). Cells were then treated with ghrelin 100 nM (in **(c)**, cells were treated with 0.5 μM forskolin (FK)). ERK1/2 phosphorylation (**(d)**) was analyzed using an AlphaScreen®SureFire® kit (Perkin Elmer). Fluorescence of the GCaMP6 sensor was used to monitor cytosolic calcium mobilization (**(e)**), and real-time label-free DMR tracings (**(f)**) representing the picometer shifts of reflected light wavelength were recorded in an EnSpire® Multimode Plate Reader (PerkinElmer, Waltham, MA, USA). Values are the mean \pm S.E.M. from eight to 11 different experiments. One-way ANOVA followed by Dunnett's *post hoc* test showed a significant effect of treatments versus forskolin (cAMP assays, **(c)**) or control (pERK1/2 assays, **(d)**), and one-way ANOVA followed by Bonferroni's *post hoc* test showed a significant effect of treatments versus ghrelin, $##p < 0.01$ and $###p < 0.001$



Cocaine Inhibits GHS-R1a Signaling

We first evaluated the effect of cocaine and PRE-084 on GHS-R1a-mediated signaling by measuring cAMP levels. HEK-293T cells endogenously express σ_1R , but do not express ghrelin receptors [35]. Moreover, it is known that low concentrations of GHS-R1b expression significantly increase GHS-R1a signaling [21]. Thus, to analyze GHS-R1a signaling pathways in HEK-293T cells, we co-expressed GHS-R1a (1.66 μ g cDNA) with low amounts of GHS-R1b (0.25 μ g cDNA). Stimulation of these cells with ghrelin (100 nM) in the presence of forskolin (0.5 μ M) significantly decreased cAMP levels (Fig. 3c). This agrees with the previously reported coupling of ghrelin receptors with G_i (

www.guidetopharmacology.org) [7]. The effect of ghrelin on forskolin-induced cAMP levels was completely blocked by pretreatment with the GHS-R1a selective antagonist YIL-781 (2 μ M) (Fig. 3c). Interestingly, when cells were treated with cocaine (30 μ M, 15 min) or the σ_1 R agonist (PRE-084, 100 nM, 15 min) prior to ghrelin stimulation, the decrease in cAMP levels was prevented to the extent similar to the one occurring with the GHS-R1a selective antagonist YIL-781 (Fig. 3c). This suggests that cocaine behaves as agonist of σ_1 R and inhibits GHS-R1a signaling as efficiently as the GHS-R1a selective antagonist YIL-781 bound to the orthosteric binding site. Similar experiments were carried out in HEK-293T transfected with another class A GPCR. When the adenosine A_1 R receptors were used instead of ~~instead of~~ GHS-R1a, neither ghrelin, nor cocaine induced any effect (Supplementary Fig. 2A-B). Moreover, A_1 adenosine receptor expressing HEK-293T cells treated with a selective agonist (R-PIA, 100 nM) showed a significant decrease in cAMP and increase in MAPK phosphorylation that was abolished by the A_1 receptor antagonist (1 μ M, DPCPX) but not by cocaine or PRE-084 (Supplementary Fig. 2C-D).

Measurement of ERK1/2 phosphorylation in HEK-293T cells transfected with GHS-R1a and GHS-R1b after stimulation with ghrelin shows an increase of 80% (Fig. 3d). Similarly to measurements of cAMP levels (Fig. 3c), the GHS-R1a selective antagonist YIL-781 and the σ_1 R agonists cocaine and PRE-084 inhibited ghrelin effects (Fig. 3d). This indicates that cocaine and PRE-084 not only affect the α_1 -dependent pathway, but also the $\beta\gamma$ -dependent signaling. Moreover, a characteristic trace of intracellular calcium transient levels was obtained in HEK-293T cells expressing GHS-R1a, GHS-R1b, and σ_1 R after activation with ghrelin (Fig. 3e). The calcium signal was abrogated by the selective ghrelin receptor antagonist and was reduced by cocaine and by PRE-084. To further test the inhibitory effect of agonist binding to σ_1 R in GHS-R1a, we performed dynamic mass redistribution (DMR) recordings that measure the changes in the wavelength of light passing through cell monolayer [36]. Once again, the magnitude of the signaling by ghrelin significantly decreased in the presence of YIL-781, cocaine, and PRE-084 (Fig. 3f). We can, thus, conclude that the GHS-R1a selective antagonist YIL-781, cocaine, and PRE-084 inhibited ghrelin effects, as measured by cAMP levels, ERK1/2 phosphorylation, and DMR signal.

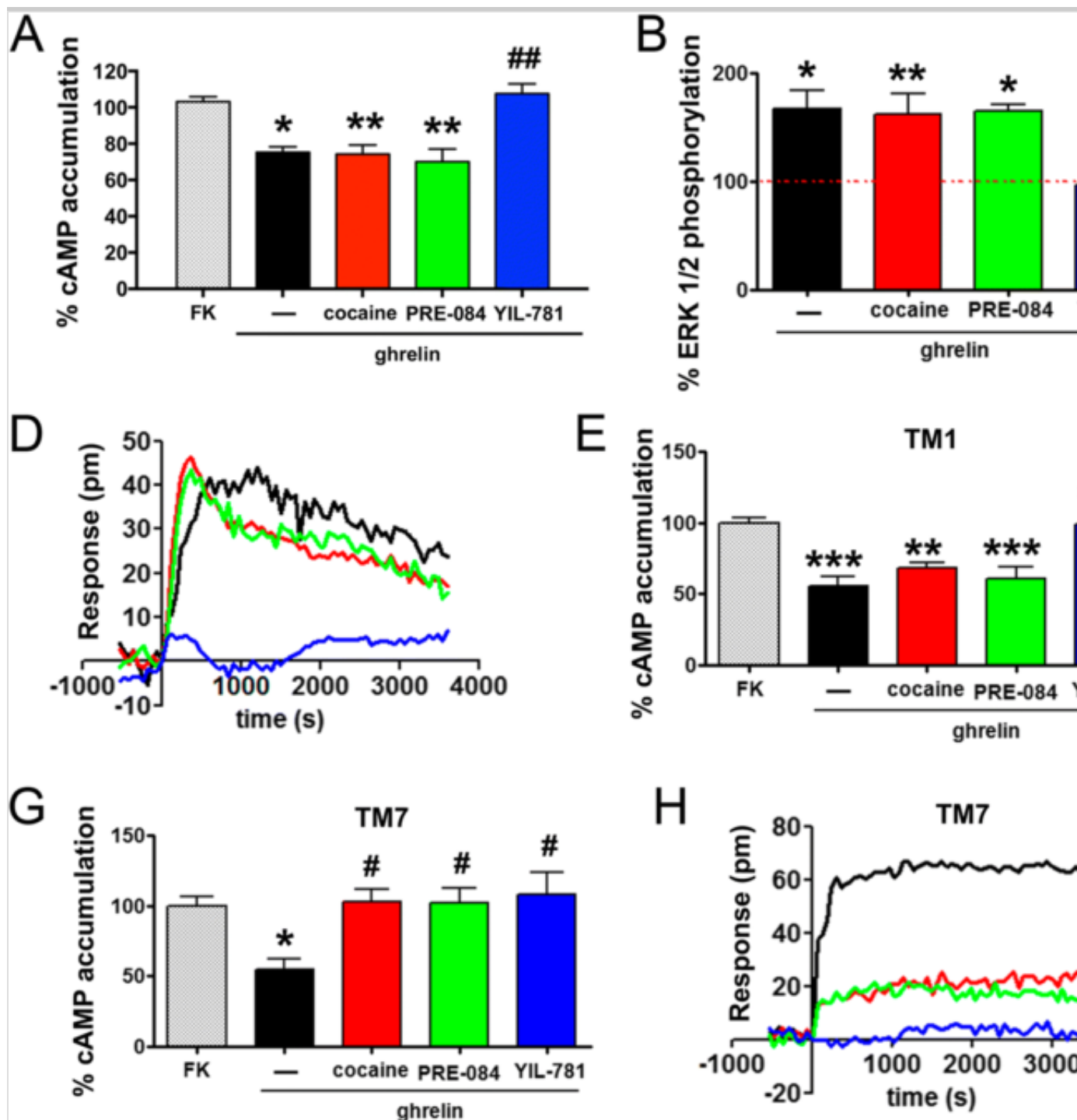
Cocaine Inhibition of GHS-R1a Signaling Is Mediated by σ_1 R

To check whether cocaine inhibition of ghrelin-induced signaling was due to its interaction with σ_1 R, HEK-293T cells expressing GHS-R1a (1.66 μ g cDNA) and GHS-R1b (0.25 μ g cDNA) were transfected with a siRNA designed to knock down expression of σ_1 R (3 μ g siRNA). Cells incorporating siRNA responded to 100 nM of ghrelin in both forskolin-induced cAMP determination and ERK1/2 phosphorylation, with similar results to those in cells without siRNA (Fig. 4a, b). However, in the presence of siRNA, cocaine or PRE-084 had no effect on ghrelin-induced signals while pretreatment with YIL-781 blocked ghrelin-induced GHS-1a activation. Also, when HEK-293T cells expressing GHS-R1a were transfected with siRNA against σ_1 R, ghrelin induced a characteristic signal on calcium mobilization or on DMR recordings. Similarly, these stimulations were not affected by cocaine or PRE-084 pretreatment, while they were completely blocked by the ghrelin antagonist YIL-781 (Fig 4c,d). These results show that cocaine effects on GHS-R1a receptor are mediated by σ_1 R.

Fig. 4

Effects of cocaine on GHS-R1a signaling are dependent on σ_1 R expression. **a–d** HEK-293T cells were transfected with 1.66 μ g GHS-R1a cDNA, 0.25 μ g GHS-R1b cDNA, and 3 μ g siRNA for σ_1 R. These cells were treated with 30 μ M of cocaine (red), 100 nM of the σ_1 R agonist, PRE-084 (green), 2 μ M of the GHS-R1a antagonist, YIL-781 (blue), or vehicle (black) followed by 100 nM of ghrelin stimulation (in **(a)**, cells were treated with 0.5 μ M forskolin). cAMP levels (**(a)**), pERK1/2 (**(b)**), calcium ion (**(c)**), and DMR (**(d)**) signals were recorded. Values are the mean \pm S.E.M. from eight to 11 different experiments. One-way ANOVA followed by Dunnett's *post hoc* test showed a significant effect of treatments versus forskolin (cAMP assays, **(a)**) or control (pERK1/2 assays, **(b)**), * $p < 0.05$, ** $p < 0.01$, and one-way ANOVA followed by Bonferroni's *post hoc* test showed a significant effect of treatments versus ghrelin, ### $p < 0.01$. **e–f** HEK-293T cells expressing GHS-R1a (0.5 μ g cDNA) were treated for 4 h with TM1 (**(e)**, **(f)**) or TM7 (**(g)**, **(h)**) TAT-peptides. Cells were subsequently treated with 30 μ M cocaine (red), 100 nM PRE-084 (green), 1 μ M YIL-781 (blue), or vehicle (black). Cells were then treated with 100 nM ghrelin ((in **(e)** and **(g)**), cells were treated with 0.5 μ M

forskolin). Traces representing DMR signal variation over time are represented in **f** and **h**. Values are the mean \pm S.E.M. of six different experiments. One-way ANOVA followed by Dunnett's *post hoc* test showed a significant effect of treatments versus forskolin, $*p < 0.05$, $**p < 0.01$, and $***p < 0.001$, and one-way ANOVA followed by Bonferroni's *post hoc* test showed a significant effect of treatments versus ghrelin, $\#p < 0.05$ and $###p < 0.001$



Disruption of the Heteromeric Complex Between σ_1 R and GHS-R1a by the TM1 Interference Peptide Blocks the Effect of Cocaine on GHS-R1a Function

As proposed above from data using TAT-fused synthetic peptides, the single TM helix of σ_1 R likely interacts with TMs 1 and 2 of GHS-R1a. Accordingly, we can hypothesize that addition of the TM1 interference peptide would abolish the effect of cocaine on GHS-R1a function. Thus, HEK-293T cells expressing GHS-R1a (1.66 μ g cDNA) were treated during 4 h with 4 μ M of TAT-TM1 (or TAT-TM7 as negative control). In agreement with our hypothesis, disruption of σ_1 R-GHS-R1a heteromeric complex was achieved by TM1, but not by TM7 TAT peptides; in these experimental conditions in which TM1 peptide was present, only the GHS-R1a selective antagonist YIL-781 (1 μ M) blocked ghrelin (100 nM) stimulation, whereas cocaine (30 μ M) or PRE-084 (100 nM) did not display any effect on either cAMP levels (Fig. 4e, g) or DMR signals (Fig. 4f, h). These results demonstrate that disruption of the GHS-R1a- σ_1 R interaction using TM1 alters the cocaine effect on ghrelin receptors, thus reinforcing the idea that cocaine modulates GHS-R1a receptor function via σ_1 R.

Next, we attempted to provide insight into the mechanism by which cocaine binds to σ_1 R and blocks GHS-R1a function. Our structural model predicts that a single protomer of GHS-R1a cannot simultaneously bind σ_1 R (via the TM 1/2 interface) and G_i (supplementary Fig. S1); accordingly, σ_1 R may impede G_i binding and, in consequence, GHS-R1a function. However, this does not seem reasonable due to the possible formation of a GHS-R1a homodimer in which one protomer binds G_i and the second protomer binds σ_1 R (Fig. 2h). Notably, this model positions the cytoplasmic domain of one protomer of the σ_1 R trimeric structure near the α -helical domain (α AH) of the G protein α -subunit (Fig. 2h). It has been shown that the mechanism for receptor-catalyzed nucleotide exchange in G proteins involves a large-scale opening of α AH, from the *Ras* domain, allowing GDP to freely dissociate [37]. This opening of α AH is not feasible in the presence of the σ_1 R trimeric structure bound to TMs 1 and 2 of GHS-R1a. Modification of the GHS-R1a- σ_1 R interaction, by inserting the TAT-fused TM1 peptide, would increase the distance between cytoplasmic domain of σ_1 R and α AH, facilitating G_i function, and these were the results found in our assays.

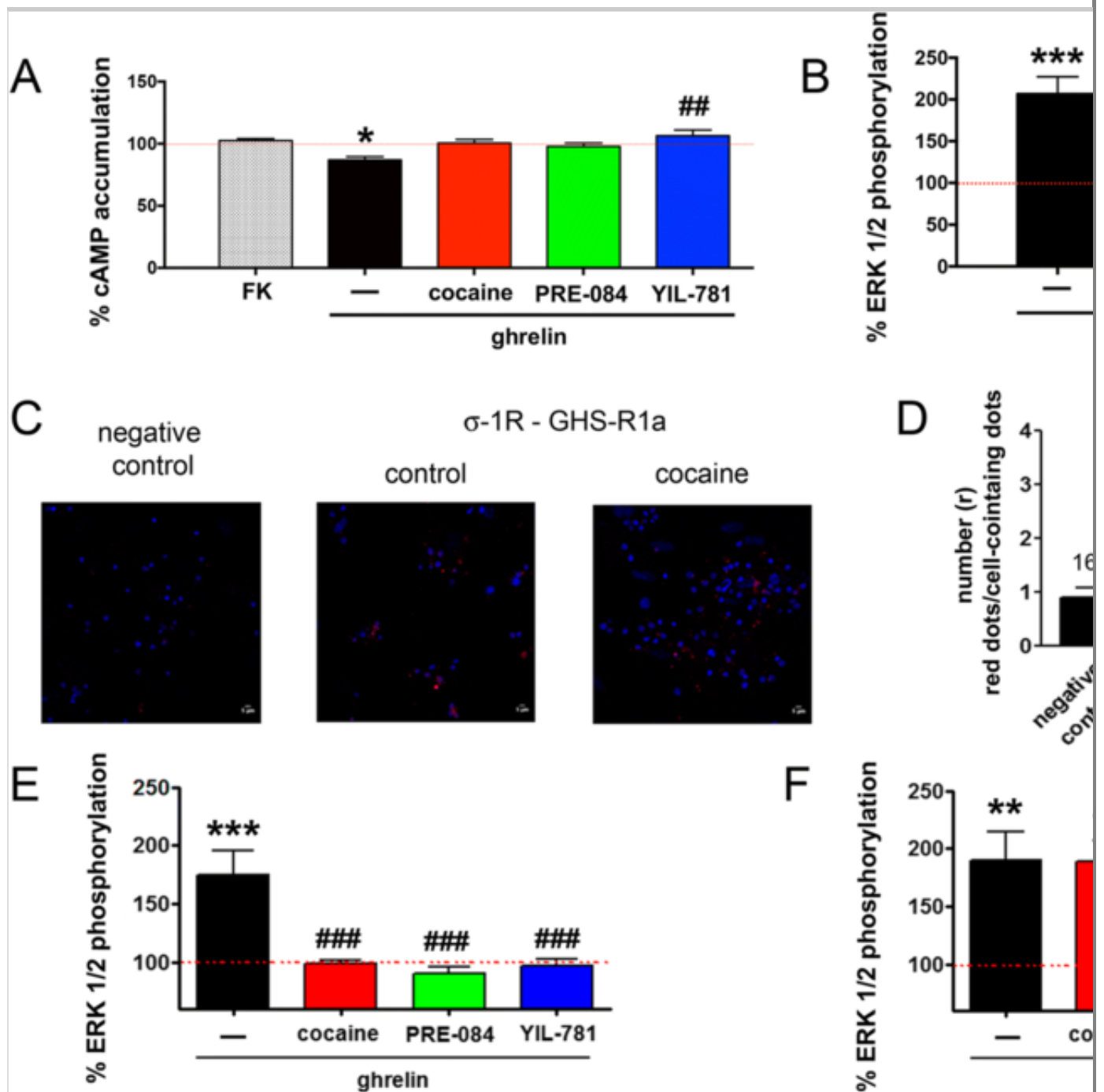
Effect of Cocaine Treatment on a Cell Line and on Primary Cultures of Striatal Neurons

Most of the cocaine effects in the central nervous system (CNS) occur in the striatum [38, 39]. Consequently, we analyzed cocaine effects on GHS-R1a expressed in the SH-SY5Y neuroblastoma cell line. Cells were transfected with cDNAs for GHS-R1a (1.66 μ g), GHS-R1b (0.25 μ g), and σ_1 R (0.75 μ g). The results were similar to those obtained in HEK-293T cells, i.e., cocaine and PRE-084 specifically blocked ghrelin action on cAMP levels and ERK1/2 phosphorylation (Fig. 5a, b). Pretreatment with the ghrelin receptor antagonist, YIL-781, also blocked ghrelin effects in neuroblastoma cells. Then, we moved to primary cultures of striatal neurons to analyze in a more physiological environment the cocaine effects over GHS-R1a receptors. The in situ proximity ligation assay (PLA), which allows the identification of interactions between two proteins in close proximity (< 17 nm) [10, 40, 41] was used to identify GHS-R1a- σ_1 R complexes, detected as punctate red marks surrounding Hoechst-stained nuclei (Fig. 5a). In striatal primary cultures, 43% of cells presented red dots with two dots/cell-containing dots. However, when these cells were treated with 30 μ M cocaine for 30 min, the number of cells containing red dots and the **number ratio** of dots/cell-containing dots increased significantly (54% of cells presented red dots with 3.2 dots/cell-containing dots). These results indicate that cocaine pretreatment increases GHS-R1a- σ_1 R complex **formation expression** in striatal primary cultures (Fig. 5a, b). Cocaine effects on GHS-R1a signaling were further analyzed in primary cultures of striatal neurons, both in cAMP level determination and in ERK1/2 phosphorylation assays. Cocaine and PRE-084 counteracted the **ghrelin-induced ghrelin-induction-of** GHS-R1a signaling in a similar way as the GHS-R1a-specific antagonist YIL-781 (Fig. 5c, d). Such effect of cocaine was related to σ_1 R modulation of GHS-R1a, as in striatal primary cultures treated with siRNA for σ_1 R, neither cocaine nor PRE-084 achieved any significant effect (Fig. 5e, f).

Fig. 5

Cocaine treatment inhibited GHS-R1a signaling in primary cultures of striatal neurons. **a, b** SH-SY5Y cells were transfected with cDNAs for GHS-R1a (1.66 μ g), GHS-R1b (0.25 μ g), and σ_1 R (0.75 μ g). Assays were performed in transfected cells treated with 30 μ M cocaine (red) cocaine, 100 nM of the σ_1 R

agonist, PRE-084 (green), 2 μ M of the GHS-R1a antagonist, YIL-781 (blue), or vehicle (black) prior to 100 nM ghrelin addition. cAMP levels were determined after 15 min of 0.5 μ M forskolin treatment (**a**). ERK1/2 phosphorylation (**b**) was determined using an AlphaScreen®SureFire® kit (Perkin Elmer). Values are \pm S.E.M. from five to six different experiments. One-way ANOVA followed by Dunnett's *post hoc* test showed a significant effect of treatments versus forskolin (cAMP assay) or versus control (ERK phosphorylation assay), $*p < 0.05$, $**p < 0.01$, and $***p < 0.001$, and one-way ANOVA followed by Bonferroni's *post hoc* test showed a significant effect of treatments versus ghrelin, $##p < 0.01$ and $###p < 0.001$. In **c**, **d**, GHS-R1a- σ_1 R heteroreceptor complexes were identified in striatal primary cultures treated with 30 μ M cocaine, 100 nM PRE-084, or vehicle and detected by PLA (see "Methods") using a polyclonal anti- σ_1 R primary antibody (1/100, Santa Cruz Biotechnology, Dallas, US) and a polyclonal anti-ghrelin primary antibody (1/100, AbCam, Cambridge, UK). Nuclei were labeled using Hoechst (1/100). **c** Representative confocal images showing GHS-R1a- σ_1 R complexes as red dots surrounding Hoechst-stained nuclei. Scale bar, 5 μ m. **d** Percentage of positive cells (containing one or more red dots in cells in five–six different fields), and number (*r*) of red dots/cell-containing dots in primary cultures of striatal neurons. One-way ANOVA followed by Dunnett's *post hoc* test showed a significant effect of treatments versus the negative control, $*p < 0.05$, $**p < 0.01$, and one-way ANOVA followed by Bonferroni's *post hoc* test showed a significant effect of treatments versus the untreated cells, $#p < 0.05$. **e**, **f** Striatal primary cultures transfected (**f**) or not (**e**) with 3 μ g siRNA for σ_1 R were treated with 30 μ M cocaine (red), 100 nM of the σ_1 R agonist, PRE-084 (green), 2 μ M of the GHS-R1a antagonist, YIL-781 (blue), or vehicle (black) prior to 100 nM ghrelin addition. ERK1/2 phosphorylation (**e**, **f**) was analyzed using an AlphaScreen®SureFire® kit (Perkin Elmer). Values are \pm S.E.M. from six to eight different experiments. One-way ANOVA followed by Dunnett's *post hoc* test showed a significant effect of treatments versus control, $*p < 0.05$, $**p < 0.01$, and $***p < 0.001$, and one-way ANOVA followed by Bonferroni's *post hoc* test showed a significant effect of treatments versus ghrelin, $###p < 0.001$



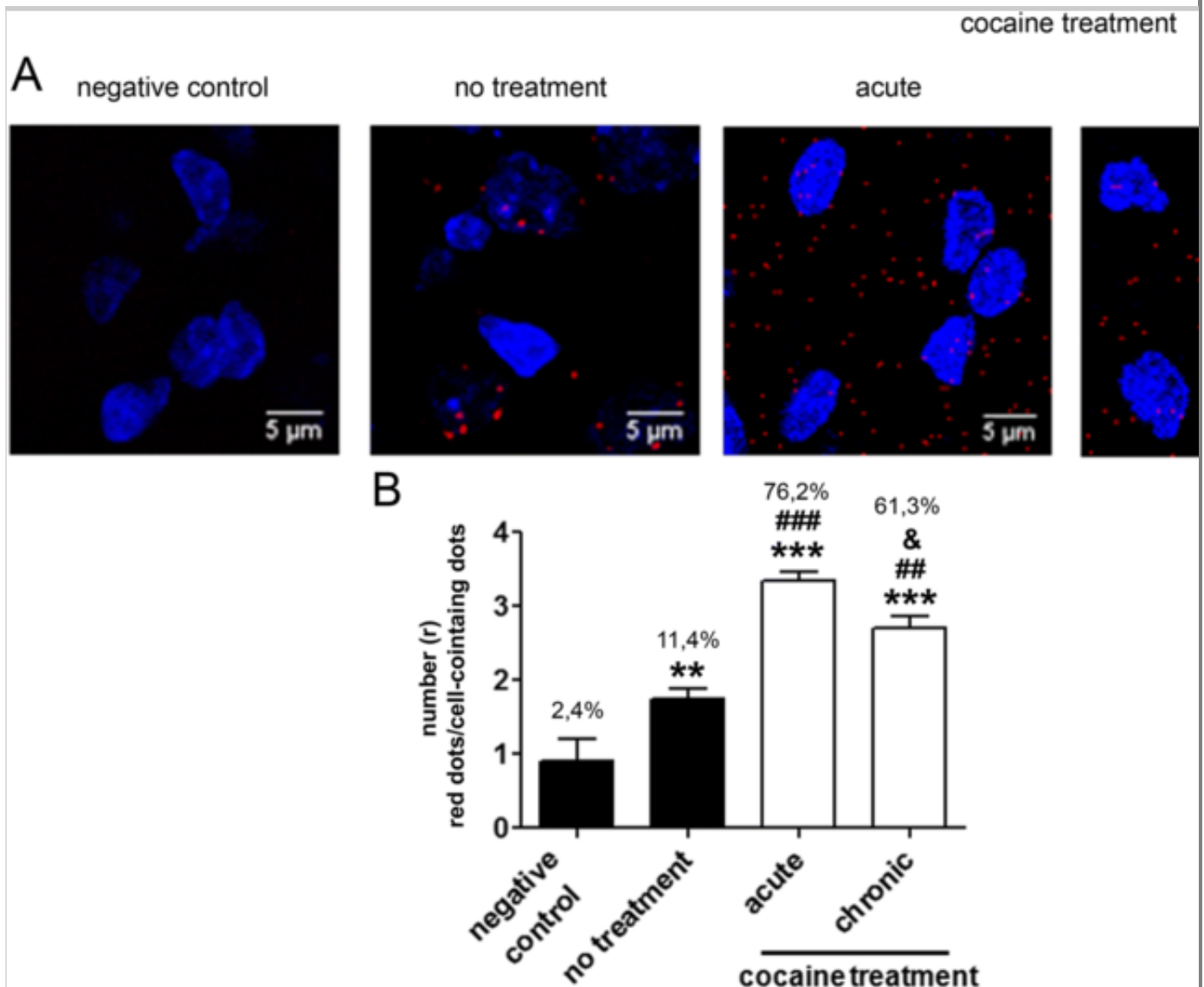
Effect of Cocaine Administration on GHS-R1a- σ ₁R Heteromer Expression in Striatal Sections from Naïve and Cocaine-Treated Animals

Following i.p. administration of 15 mg/kg cocaine for 1 (acute) or 14 (chronic) days, rats were sacrificed, and 30 μ m thick striatal sections were obtained from each group of animals and from vehicle-treated animals. The in situ proximity ligation assay (PLA) was used to identify GHS-R1a- σ ₁R heteroreceptor complexes (Fig. 6a). When striatal sections of vehicle-treated animals were

analyzed, it was observed that 11% of cells showed red dots with 1.6 dots/cell-containing dots (Fig. 6b), indicating that around 10% of striatal cells expressed GHS-R1a- σ_1 R complexes. Interestingly, in the case of the chronic treatment, the number of cells containing dots strongly increased to 61%, and also, the number of dots/cell-containing dots (2.7) was significantly higher compared to control cells. Remarkably, the cocaine acute treatment leads to values that were even higher than in the chronic condition (76% of cells containing dots and 3.2 dots/cell-containing dots). These results indicate that cocaine treatment modulated GHS-R1a- σ_1 R complex formation in striatal rat sections with a maximum increase in heteromer formation found in acute conditions (Fig. 6b).

Fig. 6

Acute and chronic cocaine treatment increase the GHS-R1a- σ_1 R heteromer expression in the rat striatum. Male Sprague-Dawley rats were i.p. administrated with vehicle (control) or 15 mg/kg cocaine for 1 (acute) or 14 (chronic) days. To identify σ_1 -GHS-R1a complexes from each condition, rats were sacrificed and 30 μ m thick striatal sections were obtained and treated with a polyclonal anti- σ_1 R primary antibody (1/100, Santa Cruz Biotechnology, Dallas, US) and a polyclonal anti-ghrelin primary antibody (1/100, AbCam, Cambridge, UK) in the presence of Hoechst (1/100) and then treated with the PLA probes (see “Methods”). Representative PLA confocal images showing GHS-R1a- σ_1 R complexes as red dots surrounding Hoechst-stained nuclei are shown for each condition (Fig. 6a). Scale bar, 5 μ m. **b** Percentage of positive cells (containing one or more red dots; from cells in four–six different fields) and number (*r*) of red dots/cell-containing dots in rat striatal sections. One-way ANOVA followed by Dunnett’s *post hoc* test showed a significant effect of treatments versus the negative control, **p* < 0.05, ***p* < 0.01, one-way ANOVA followed by Bonferroni’s *post hoc* test showed a significant effect of treatments versus the untreated cells, ###*p* < 0.001, and one-way ANOVA followed by Bonferroni’s *post hoc* test showed a significant effect of chronic treatment versus acutely treated sections, &*p* < 0.05



Discussion

The endogenous ligand of σ_1 R remains unknown; however, synthetic agonists and antagonists are available. PRE-084 is a selective agonist due to its ability to dose-dependently dissociate σ_1 R from a binding immunoglobulin protein/78 kDa glucose-regulated protein (BiP/GPR-78) [42]. Despite not being associated with a specific signaling machinery, σ_1 R operates via translocation to the plasma membrane and via protein-protein-mediated modulation of cell responses upon agonist activation [11]. The mechanism involves calcium signaling and ion channel activation [43]; and, in addition, to the regulation of GPCR's function [11]. For instance, it has been shown that σ_1 R is involved in the negative control that glutamate N-methyl-D-aspartate acid receptors (NMDARs) exert on opioid antinociception (Rodríguez-Muñoz et al. 2015). Thus, σ_1 R

antagonists would enhance antinociception and reduce neuropathic pain induced by μ -opioid receptors. Another remarkable example is the control of σ_1 R in the interaction between cannabinoid CB1 and NMDA~~R~~ receptors, whose ~~failure~~ **functional unbalance** constitutes a vulnerability factor for cannabis abuse, potentially precipitating schizophrenia [44]. Upon demonstrating that cocaine binds to σ_1 R even at doses attained at recreational use, σ_1 R is proposed to mediate locomotor activation [45, 46], seizures [18], drug sensitization [47], and reward actions [48, 49]. Reduction of σ_1 R levels by injection of antisense nucleotides results in attenuating the convulsive effects of the drug [50], whereas the action of σ_1 R agonists or antagonists exacerbates or minimizes, respectively, cocaine effects [50, 51, 52]. Although activation of σ_1 R by agonists is also involved in the appetitive properties of cocaine [49], the underlying mechanism remains unknown. In this manuscript, we reveal for the first time that σ_1 Rs mediate the ~~hunger-suppressive~~ **hunger-suppressive** action of cocaine by interacting with orexigenic ghrelin receptors.

The nucleus accumbens, one of the structures that form the striatum, is part of the reward system. Activation of this system in response to food intake produces a pleasant sensation and other primordial needs for mammalian survival [53]. It should be noted that in these mesolimbic regions, GHS-R1a is co-expressed in neurons with cocaine-sensitive σ_1 R. From both mechanistic and molecular point of views, this report highlights an interaction between σ_1 R and GHS-R1a that is translated into a strong inhibition of ghrelin-induced GHS-R1a signaling, as measured by G protein-dependent (cAMP accumulation and calcium release assays) and **partly/fully** G protein-independent (MAPK phosphorylation and dynamic mass redistribution assays) signaling pathways. We have shown in transfected HEK-293T cells and in striatal primary cultures of neurons that pretreatment with the σ_1 R agonists cocaine or PRE-084 inhibits ghrelin-mediated signaling in a similar manner as the GHS-R1a antagonist YIL-781. This effect is mediated by σ_1 R, because, in σ_1 R-siRNA-treated cells, cocaine or PRE-084 had no effect on ghrelin-induced signals while the ghrelin receptor antagonist, YIL-781, maintained its effect.

Kotagale and collaborators [54] have described the potent orexigenic effects of neuropeptide Y (NPY), which was described in autoradiographic studies [55] as a possible endogenous ligand for a subpopulation of sigma receptors, thus

linking the stimulation of sigma receptors with hunger. It turned out that the action of NPY on sigma receptors could not be reproduced, i.e., no high affinity binding of NPY to brain sigma receptors can be measured [56]. Our results show that cocaine binding to σ_1 R could counteract the feeling of hunger by a mechanism that excludes a direct competition between cocaine and NPY to interact with σ_1 R. The proposed formation of the σ_1 R-GHS-R1a interaction becomes even more important by the finding that heteromer expression is increased in both acute and chronic cocaine administration. However, the effect was more marked in acute conditions. In fact, striatal sections of Sprague-Dawley rats injected for 1 day with 15 mg/kg cocaine displayed threefold higher expression of σ_1 R-GHS-R1a heteromers than the control animals.

The structure of σ_1 R has traditionally considered to be formed by two TM helices. However, the recently released crystal structure of σ_1 R has shown **homotrimers whose protomers contain** a single TM domain and a C-terminal **tail domain** having a buried ligand-binding site ~~that arranges into homotrimers~~ [25]. We have proposed, **from data** using TAT-fused synthetic peptides together with BiFC assays, that this single TM helix of **one σ_1 R molecule** can be recognized by two different interacting interfaces of the 7TM bundle of **GHS-R1a GPCRs**, either by interfaces formed by TMs 1 and 2 or TMs 5 and 6. Oligomerization of GPCRs via a particular interface likely guides the interacting interface in the σ_1 R. **The same TM helices may be involved in interactions of σ_1 R with other GPCRs.** In the particular case of σ_1 R-GHS-R1a, due to the formation of the GHS-R1a-GHS-R1b heterotetramer via TM 4/5 and TM 5/6 interfaces, σ_1 R can interact with GHS-R1a via the free TM 1/2 interface. We would like to speculate that, because σ_1 R is a homotrimer, the two additional TM helices can bind two additional GHS-R1a-GHS-R1b heterotetramers, suggesting the possible **existence occurrence** of higher order complexes **formed by between** GHS-R1a and σ_1 R, produced by ~~the~~ successive combination of these units. These clusters may form specialized machineries of σ_1 R-mediated signaling.

Funding Information

This work was supported by **a grants** from the Spanish Ministry of Innovation and Competitiveness (MINECO Ref. No. BFU2015-664405-R, **SAF2015-74627-JIN and SAF2016-77830-R**; ~~it~~ **they** may include FEDER European

Union funds).

Compliance with Ethical Standards

Conflict of Interest The authors declare that they have no conflict of interests.

Electronic supplementary material

Supplementary Figure 1

Effect of interfering peptides on the σ_1 R-GHS-R1a expression in HEK-293 T cells. Panel A: BiFC complementation experiments were performed in HEK-293 T cells transfected with 0.75 μ g cDNA for GHS-R1a-nYFP and 0.75 μ g cDNA for σ_1 R-cYFP (right panel). Fluorescence due to reconstituted YFP was detected in a Leica SP2 microscope. Nuclei were stained with Hoechst (1/100). As negative control (left panel), BiFC complementation experiments were performed in HEK-293 T cells transfected only with 0.75 μ g cDNA for σ_1 R-cYFP. Scale bar 5 μ m. Panel B: PLA assays in HEK-293 T cells expressing σ_1 R (0.75 μ g of plasmid) and GHS-R1a (1.66 μ g of plasmid) treated for 4 h with TM1, TM2 or TM7 TAT peptides prior to incubation with a polyclonal anti- σ_1 R primary antibody (1/100, Santa Cruz Biotechnology, Dallas, US) and a polyclonal anti-ghrelin primary antibody (1/100, AbCam, Cambridge, UK). Nuclei were labeled using Hoechst (1/100). GHS-R1a- σ_1 R complexes are shown as red dots surrounding Hoechst-stained nuclei. Scale bar 10 μ m. (GIF 283 kb)



[High resolution image \(TIF 15132 kb\)](#) Missing all Supplementary figs. Do you need them?

Supplementary Figure 2

Effects of cocaine on A_1 adenosine receptor-mediated signaling. In A-D, HEK-293 T cells were transfected with 1 μ g of cDNA for A_1 R and 0.75 μ g cDNA for σ_1 R-YFP and treated with 30 μ M of cocaine (red), 100 nM of the σ_1 R agonist,

PRE-084 (green), 2 μ M of the GHS-R1a antagonist, YIL-781 (blue), (A,B) or the A₁R antagonist (1 μ M DPCPX, pink) (C,D) or vehicle (black). Cells were then treated with 100 nM ghrelin (A,B) or the A₁R agonist (100 nM R-PIA). In panels A and C, cells were treated with 0.5 μ M forskolin (FK) prior to cAMP level determination. ERK1/2 phosphorylation (B and D) was analyzed using an AlphaScreen®SureFire® kit (Perkin Elmer). Values are the mean \pm S.E.M. from 6 to 8 different experiments. One-way ANOVA followed by Dunnett's *post-hoc* test showed a significant effect of treatments versus forskolin (cAMP assays, panel A, C) or control (pERK1/2 assays, panel B, D), * $p < 0.05$ and *** $p < 0.001$. (GIF 114 kb)



Hight resolution image (TIF 2341 kb)

References

1. Howick K, Griffin B, Cryan J, Schellekens H (2017) From belly to brain: targeting the ghrelin receptor in appetite and food intake regulation. *Int J Mol Sci* 18:273. <https://doi.org/10.3390/ijms18020273>
2. Cassidy RM, Tong Q (2017) Hunger and satiety gauge reward sensitivity. *Front Endocrinol (Lausanne)* 8:104. <https://doi.org/10.3389/fendo.2017.00104>
3. Conn PM, Bowers CY (1996) A new receptor for growth hormone-release peptide. *Science* 273:923–920
4. Geelissen SME, Beck IME, Darras VM, Kühn ER, van der Geyten S (2003) Distribution and regulation of chicken growth hormone secretagogue receptor isoforms. *Gen Comp Endocrinol* 134:167–174
5. Chan C-B, Cheng CH (2004) Identification and functional

characterization of two alternatively spliced growth hormone secretagogue receptor transcripts from the pituitary of black seabream *Acanthopagrus schlegelii*. *Mol Cell Endocrinol* 214:81–95.
<https://doi.org/10.1016/j.mce.2003.11.020>

6. Mary S, Fehrentz J-A, Damian M, Gaibelet G, Orcel H, Verdié P, Mouillac B, Martinez J et al (2013) Heterodimerization with its splice variant blocks the ghrelin receptor 1a in a non-signaling conformation: a study with a purified heterodimer assembled into lipid discs. *J Biol Chem* 288:24656–24665. <https://doi.org/10.1074/jbc.M113.453423>

7. Navarro G, Aguinaga D, Angelats E, Medrano M, Moreno E, Mallol J, Cortés A, Canela EI et al (2016) A significant role of the truncated ghrelin receptor GHS-R1b in ghrelin-induced signaling in neurons. *J Biol Chem* 291:13048–13062. <https://doi.org/10.1074/jbc.M116.715144>

8. Chow KBS, Sun J, Chu KM et al (2012) The truncated ghrelin receptor polypeptide (GHS-R1b) is localized in the endoplasmic reticulum where it forms heterodimers with ghrelin receptors (GHS-R1a) to attenuate their cell surface expression. *Mol Cell Endocrinol* 348:247–254.
<https://doi.org/10.1016/j.mce.2011.08.034>

9. Damian M, Mary S, Maingot M, M'Kadmi C, Gagne D, Leyris JP, Denoyelle S, Gaibelet G et al (2015) Ghrelin receptor conformational dynamics regulate the transition from a preassembled to an active receptor:Gq complex. *Proc Natl Acad Sci* 112:1601–1606.
<https://doi.org/10.1073/pnas.1414618112>

10. Borroto-Escuela DO, Brito I, Romero-Fernandez W, di Palma M, Oflijan J, Skieterska K, Duchou J, van Craenenbroeck K et al (2014) The G protein-coupled receptor heterodimer network (GPCR-HetNet) and its hub components. *Int J Mol Sci* 15:8570–8590.
<https://doi.org/10.3390/ijms15058570>

11. Su TP, Su TC, Nakamura Y, Tsai SY (2016) The Sigma-1 receptor as a pluripotent modulator in living systems. *Trends Pharmacol Sci* 37:262–278.

<https://doi.org/10.1016/j.tips.2016.01.003>

12. Corbera J, Vaño D, Martínez D, Vela JM, Zamanillo D, Dordal A, Andreu F, Hernandez E et al (2006) A medicinal-chemistry-guided approach to selective and druglike sigma-1 ligands. *ChemMedChem* 1:140–154.

<https://doi.org/10.1002/cmdc.200500034>

13. Mei J, Pasternak GW (2002) Sigma1 receptor modulation of opioid analgesia in the mouse. *J Pharmacol Exp Ther* 300:1070–1074

14. Sun H, Shi M, Zhang W, Zheng YM, Xu YZ, Shi JJ, Liu T, Gunosewoyo H et al (2016) Development of novel alkoxyisoxazoles as sigma-1 receptor antagonists with antinociceptive efficacy. *J Med Chem* 59:6329–6343.

<https://doi.org/10.1021/acs.jmedchem.6b00571>

15. McCracken KA, Bowen WD, de Costa BR, Matsumoto RR (1999) Two novel sigma receptor ligands, BD1047 and LR172, attenuate cocaine-induced toxicity and locomotor activity. *Eur J Pharmacol* 370:225–232

16. Skuza G (1999) Effect of sigma ligands on the cocaine-induced convulsions in mice. *Pol J Pharmacol* 51:477–483

17. Lever JR, Fergason-Cantrell EA, Watkinson LD, Carmack TL, Lord SA, Xu R, Miller DK, Lever SZ (2016) Cocaine occupancy of sigma₁ receptors and dopamine transporters in mice. *Synapse* 70:98–111.

<https://doi.org/10.1002/syn.21877>

18. Matsumoto RR, Hewett KL, Pouw B, Bowen WD, Husbands SM, Cao JJ, Hauck Newman A (2001) Rimcazole analogs attenuate the convulsive effects of cocaine: correlation with binding to sigma receptors rather than dopamine transporters. *Neuropharmacology* 41:878–886.

[https://doi.org/10.1016/S0028-3908\(01\)00116-2](https://doi.org/10.1016/S0028-3908(01)00116-2)

19. Marcellino D, Navarro G, Sahlholm K, Nilsson J, Agnati LF, Canela EI, Lluís C, Århem P et al (2010) Cocaine produces D2R-mediated conformational changes in the adenosine A(2A)R-dopamine D2R heteromer.

Biochem Biophys Res Commun 394:988–992.

<https://doi.org/10.1016/j.bbrc.2010.03.104>

20. Navarro G, Moreno E, Bonaventura J, Brugarolas M, Farré D, Aguinaga D, Mallol J, Cortés A et al (2013) Cocaine inhibits dopamine D2 receptor signaling via sigma-1-D2 receptor heteromers. PLoS One 8:e61245.

<https://doi.org/10.1371/journal.pone.0061245>

21. Navarro G, Quiroz C, Moreno-Delgado D, Sierakowiak A, McDowell K, Moreno E, Rea W, Cai NS et al (2015) Orexin-corticotropin-releasing factor receptor heteromers in the ventral tegmental area as targets for cocaine. J Neurosci 35:6639–6653.

<https://doi.org/10.1523/JNEUROSCI.4364-14.2015>

22. Cordoní A, Navarro G, Aymerich MS, Franco R (2015) Structures for G-protein-coupled receptor tetramers in complex with G proteins. Trends Biochem Sci 40:548–551.

<https://doi.org/10.1016/j.tibs.2015.07.007>

23. Schmidt HR, Zheng S, Gurpinar E, Koehl A, Manglik A, Kruse AC (2016) Crystal structure of the human σ_1 receptor. Nature 532:527–530.

<https://doi.org/10.1038/nature17391>

24. Liu J, Yu B, Orozco-Cabal L, Grigoriadis DE, Rivier J, Vale WW, Shinnick-Gallagher P, Gallagher JP (2005) Chronic cocaine administration switches corticotropin-releasing Factor2 receptor-mediated depression to facilitation of glutamatergic transmission in the lateral septum. J Neurosci 25:577–583.

<https://doi.org/10.1523/JNEUROSCI.4196-04.2005>

25. Schmidt HR, Zheng S, Gurpinar E, Koehl A, Manglik A, Kruse AC (2016) Crystal structure of the human σ_1 receptor. Nature 532:527–530.

<https://doi.org/10.1038/nature17391>

26. Egloff P, Hillenbrand M, Klenk C, Batyuk A, Heine P, Balada S, Schlinkmann KM, Scott DJ et al (2014) Structure of signaling-competent neurotensin receptor 1 obtained by directed evolution in Escherichia coli. Proc Natl Acad Sci 111:E655–E662.

<https://doi.org/10.1073/pnas.1317903111>

27. Krumm BE, White JF, Shah P, Grisshammer R (2015) Structural prerequisites for G-protein activation by the neurotensin receptor. *Nat Commun* 6:7895. <https://doi.org/10.1038/ncomms8895>
28. Rasmussen SGF, DeVree BT, Zou Y et al (2011) Crystal structure of the β 2 adrenergic receptor-Gs protein complex. *Nature* 477:549–555. <https://doi.org/10.1038/nature10361>
29. Tesmer JJ, Berman DM, Gilman AG, Sprang SR (1997) Structure of RGS4 bound to AIF4-activated G(i alpha1): stabilization of the transition state for GTP hydrolysis. *Cell* 89:251–261
30. Manglik A, Kruse AC, Kobilka TS, Thian FS, Mathiesen JM, Sunahara RK, Pardo L, Weis WI et al (2012) Crystal structure of the μ -opioid receptor bound to a morphinan antagonist. *Nature* 485:321–326. <https://doi.org/10.1038/nature10954>
31. van Zundert GCP, Rodrigues JPGLM, Trellet M, Schmitz C, Kastiris PL, Karaca E, Melquiond ASJ, van Dijk M et al (2016) The HADDOCK2.2 web server: user-friendly integrative modeling of biomolecular complexes. *J Mol Biol* 428:720–725. <https://doi.org/10.1016/j.jmb.2015.09.014>
32. Ng GYK, O'Dowd BF, Lee SP et al (1996) Dopamine D2 receptor dimers and receptor-blocking peptides. *Biochem Biophys Res Commun* 227:200–204. <https://doi.org/10.1006/bbrc.1996.1489>
33. Hebert TE, Moffett S, Morello JP, Loisel TP, Bichet DG, Barret C, Bouvier M (1996) A peptide derived from a beta2-adrenergic receptor transmembrane domain inhibits both receptor dimerization and activation. *J Biol Chem* 271:16384–16392
34. Maurice T, Romieu P (2004) Involvement of the sigma1 receptor in the appetitive effects of cocaine. *Pharmacopsychiatry* 37(Suppl 3):S198–S207. <https://doi.org/10.1055/s-2004-832678>
35. Navarro G, Moreno E, Aymerich M, Marcellino D, McCormick PJ, Mallol J, Cortes A, Casado V et al (2010) Direct involvement of sigma-1

receptors in the dopamine D1 receptor-mediated effects of cocaine. *Proc Natl Acad Sci U S A* 107:18676–18681.

<https://doi.org/10.1073/pnas.1008911107>

36. Grundmann M, Kostenis E (2015) Holistic methods for the analysis of cNMP effects. In: *Handb. Exp. Pharmacol.* pp 339–357

37. Dror RO, Mildorf TJ, Hilger D, Manglik A, Borhani DW, Arlow DH, Philippsen A, Villanueva N et al (2015) SIGNAL TRANSDUCTION. Structural basis for nucleotide exchange in heterotrimeric G proteins. *Science* 348:1361–1365. <https://doi.org/10.1126/science.aaa5264>

38. Joffe ME, Grueter BA (2016) Cocaine experience enhances thalamo-accumbens N-methyl-D-aspartate receptor function. *Biol Psychiatry* 80:671–681. <https://doi.org/10.1016/j.biopsych.2016.04.002>

39. Borroto-Escuela DO, Narváez M, Wydra K, Pintsuk J, Pinton L, Jimenez-Beristain A, di Palma M, Jastrzębska J et al (2017) Cocaine self-administration specifically increases A2AR-D2R and D2R-sigma1R heteroreceptor complexes in the rat nucleus accumbens shell. Relevance for cocaine use disorder. *Pharmacol Biochem Behav* 155:24–31. <https://doi.org/10.1016/j.pbb.2017.03.003>

40. Trifilieff P, Rives M-L, Urizar E, Piskorowski R, Vishwasrao H, Castrillon J, Schmauss C, Slättman M et al (2011) Detection of antigen interactions ex vivo by proximity ligation assay: endogenous dopamine D2-adenosine A2A receptor complexes in the striatum. *Biotechniques* 51:111–118. <https://doi.org/10.2144/000113719>

41. Fuxe K, Borroto-Escuela DO, Ciruela F, Guidolin D, Agnati LF (2014) Receptor-receptor interactions in heteroreceptor complexes: a new principle in biology. Focus on their role in learning and memory. *Neurosci Discov* 2:6

42. Hayashi T, Su T-P (2007) Sigma-1 receptor chaperones at the ER-mitochondrion interface regulate Ca(2+) signaling and cell survival. *Cell* 131:596–610. <https://doi.org/10.1016/j.cell.2007.08.036>

43. Wu Z, Bowen WD (2008) Role of sigma-1 receptor C-terminal segment in inositol 1,4,5-trisphosphate receptor activation: constitutive enhancement of calcium signaling in MCF-7 tumor cells. *J Biol Chem* 283:28198–28215. <https://doi.org/10.1074/jbc.M802099200>
44. Sánchez-Blázquez P, Rodríguez-Muñoz M, Herrero-Labrador R, Burgueño J, Zamanillo D, Garzón J (2014) The calcium-sensitive Sigma-1 receptor prevents cannabinoids from provoking glutamate NMDA receptor hypofunction: implications in antinociception and psychotic diseases. *Int J Neuropsychopharmacol* 17:1–13. <https://doi.org/10.1017/S1461145714000029>
45. Menkel M, Terry P, Pontecorvo M, Katz JL, Witkin JM (1991) Selective sigma ligands block stimulant effects of cocaine. *Eur J Pharmacol* 201:251–252
46. Barr JL, Deliu E, Brailoiu GC, Zhao P, Yan G, Abood ME, Unterwald EM, Brailoiu E (2015) Mechanisms of activation of nucleus accumbens neurons by cocaine via sigma-1 receptor-inositol 1,4,5-trisphosphate-transient receptor potential canonical channel pathways. *Cell Calcium* 58:196–207. <https://doi.org/10.1016/j.ceca.2015.05.001>
47. Ujike H, Kuroda S, Otsuki S (1996) Sigma receptor antagonists block the development of sensitization to cocaine. *Eur J Pharmacol* 296:123–128. [https://doi.org/10.1016/0014-2999\(95\)00693-1](https://doi.org/10.1016/0014-2999(95)00693-1)
48. Romieu P, Martin-Fardon R, Maurice T (2000) Involvement of the sigma1 receptor in the cocaine-induced conditioned place preference. *Neuroreport* 11:2885–2888
49. Romieu P, Phan VL, Martin-Fardon R, Maurice T (2002) Involvement of the sigma(1) receptor in cocaine-induced conditioned place preference: possible dependence on dopamine uptake blockade. *Neuropsychopharmacology* 26:444–455. [https://doi.org/10.1016/S0893-133X\(01\)00391-8](https://doi.org/10.1016/S0893-133X(01)00391-8)

50. Matsumoto RR, McCracken KA, Pouw B et al (2002) Involvement of sigma receptors in the behavioral effects of cocaine: evidence from novel ligands and antisense oligodeoxynucleotides. *Neuropharmacology* 42:1043–1055
51. Matsumoto RR, Liu Y, Lerner M, Howard EW, Brackett DJ (2003) Sigma receptors: potential medications development target for anti-cocaine agents. *Eur J Pharmacol* 469:1–12
52. Matsumoto RR, Gilmore DL, Pouw B, Bowen WD, Williams W, Kausar A, Coop A (2004) Novel analogs of the σ receptor ligand BD1008 attenuate cocaine-induced toxicity in mice. *Eur J Pharmacol* 492:21–26.
<https://doi.org/10.1016/j.ejphar.2004.03.037>
53. Kim HF, Hikosaka O (2015) Parallel basal ganglia circuits for voluntary and automatic behaviour to reach rewards. *Brain* 138:1776–1800.
<https://doi.org/10.1093/brain/awv134>
54. Kotagale NR, Upadhyaya M, Hadole PN, Kokare DM, Taksande BG (2014) Involvement of hypothalamic neuropeptide Y in pentazocine induced suppression of food intake in rats. *Neuropeptides* 48:133–141.
<https://doi.org/10.1016/j.npep.2014.02.003>
55. Roman FJ, Pascaud X, Duffy O, Vauche D, Martin B, Junien JL (1989) Neuropeptide Y and peptide YY interact with rat brain sigma and PCP binding sites. *Eur J Pharmacol* 174:301–302
56. Tam SW, Mitchell KN (1991) Neuropeptide Y and peptide YY do not bind to brain sigma and phencyclidine binding sites. *Eur J Pharmacol* 193:121–122